

Cite this: DOI: 10.1039/xxxxxxxxxx

Electrostatic interactions between charged dielectric particles in an electrolyte solution: constant potential boundary conditions

Ivan N. Derbenev,^{a,b} Anatoly V. Filippov,^b Anthony J. Stace,^a and Elena Besley*^a

Received Date

Accepted Date

DOI: 10.1039/xxxxxxxxxx

www.rsc.org/journalname

The problem of electrostatic interactions between colloidal particles in an electrolyte solution has been solved within the Debye-Hückel approximation using the boundary condition of constant potential. The model has been validated in two independent ways - by considering the limiting cases obtained from DLVO theory and comparison with available experimental data. The presented methodology provides the final part to complete theory of pairwise electrostatic interactions between spherical colloidal particles; one that embraces all possible chemical scenarios within the boundary conditions of constant potential and constant charge.

1 Introduction

Understanding the effect of electrostatic forces is essential in the context of soft matter science for a number of reasons. Electrostatic forces are responsible for the long range repulsive interactions, which prevent dissolved particles from immediate coagulation in colloidal solutions.¹ In contrast to van der Waals forces driving short range attraction, they can be easily modified through surface properties of the interacting particles and solvent additives.² Crucially, no universal mathematically rigorous theory of electrostatic interactions between colloidal particles exist in the literature to date. The most widely used Derjaguin-Landau-Verwey-Overbeek (DLVO) theory contains a number of assumptions and limitations,^{3,4} which can be highlighted with the following example. If the surface potential on two identical particles is low ($\Phi_{\text{surface}} < 25$ mV), the electrostatic force between them can be described within the Debye-Hückel approximation as^{1,5}

$$F = 2\pi\kappa a \epsilon_0 k_m \Phi_{\text{surface}}^2 \exp[-\kappa(R - 2a)], \quad (1)$$

where κ^{-1} is the characteristic decay length of the electrostatic potential (*i.e.* Debye length), a is the radius of the particle, R is the separation between particle centres, k_m is the dielectric constant of the medium, and ϵ_0 is the dielectric permittivity of vacuum. Eq. (1) is accurate only for surface-to-surface separations exceeding one Debye length,^{1,6} and is derived from the interaction energy between two charged plates using the Derjaguin approximation that accounts for a spherical geometry of

the problem.^{4,5} A similar approach has been used to describe the interaction between two surfaces of unequal but constant potential,⁷ and a further modification was proposed by Carnie and Chan, who combined the results of constant charge and constant potential boundary conditions within the linearized Poisson-Boltzmann (Debye-Hückel) model - charge regulation approach.⁸ This method was later modified for the non-linear Poisson-Boltzmann model.⁹ Despite their flexibility all these methods are strongly dependent on the accuracy of the Derjaguin approximation, which as stated, is based on finding the interaction energy between two parallel plates and applying a factor which approximately describes the curvature of interacting surfaces.⁵

A rigorous model of pairwise electrostatic interactions in an electrolyte solution has been previously developed within the Debye-Hückel approximation,^{10,11} in which particle charge was assumed constant and uniformly distributed over the surface. The model provided good agreement with predictions obtained by non-shielded models^{12,13} and with experimental data¹⁴ on electrostatic interactions in colloids. However, the assumption of constant surface charge density is not always valid. In this paper, we consider a rigorous model for the electrostatic interactions between two spherical colloidal particles in an electrolyte solution, where it is assumed that the potential on each particle remains constant and independent of coordinates of a surface point.

The paper has the following structure. Applicability of both constant potential and constant charge boundary conditions is first discussed within the context of the experimental parameters of particle size and electrolyte concentration. A rigorous theory that implies an explicit spherical geometry without any geometrical approximations is then introduced. Finally, the calculated results are validated using two experimental data sets: for poly(methyl methacrylate) (PMMA) spheres in hexadecane¹⁴

^a School of Chemistry, University of Nottingham, University Park, Nottingham NG7 2RD, UK. Tel: +44 115 846 8465; E-mail: Elena.Besley@nottingham.ac.uk

^b Troitsk Institute for Innovation and Fusion Research, Pushkovykh Street 12, Troitsk, Moscow 142190, Russia.

and for a pair of polystyrene latex particles in an aqueous solution of KCl.² A detailed analytical consideration of approximate models for solving the electrostatic problem based on the above model has been given previously by Filippov *et al.*⁶

2 The criterion for choosing boundary conditions

A criterion for using the boundary condition of either constant charge or constant potential on the surface of a colloidal particle can be introduced in the form of a dimensionless parameter:

$$\xi \equiv \frac{\tau_{ch} v_c}{d}, \quad (2)$$

where τ_{ch} is the characteristic relaxation time of surface charge on colloidal particles, v_c is the speed of their translational motion, and d is the characteristic inter-particle distance over which the surface charge or surface potential changes. If the particles are fixed in space or the timescale of their interaction is much greater than the characteristic relaxation time of surface charge then $\xi \ll 1$, and the boundary condition of constant potential should be applied. In the opposite case, where $\xi \gg 1$, if the charging process is much slower than the time of particle displacement through a distance equivalent to its size, the surface charge is assumed to be constant. Fig. 1 shows schematically the relation between the characteristic time of particle charging and the characteristic time of particle displacement for different values of the parameter ξ .

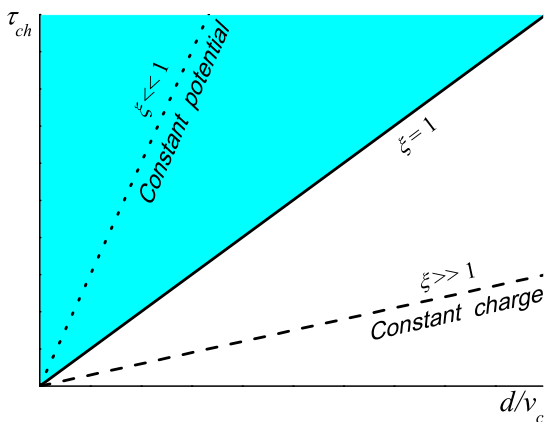


Fig. 1 Relation between the characteristic time of particle charging, τ_{ch} , and the characteristic time of particle displacement, d/v_c , for different values of the parameter ξ determining the choice of boundary condition for the electrostatic problem (constant charge or constant potential).

To quantify the criterion defined by Eq. (2), these parameters have been estimated for the solutions of sodium di-2-ethylhexylsulfosuccinate (AOT) in hexadecane and KCl in water. An electrolyte solution is a conductor, therefore, the surface potential of particles becomes equal during the Maxwell time scale¹⁵

$$\tau_{ch} \equiv \tau_M = \frac{\epsilon_0 k_m}{\zeta}, \quad (3)$$

where ζ is the conductivity of solution. Numerical simulations^{6,11,16,17} show that the characteristic length for the variation of charge at constant potential and the variation of potential at constant charges is defined by the particle radius a ; therefore,

we can set $d = a$. For v_c equal to the velocity of thermal motion of a colloidal particle, $v_c = (8k_B T / (\pi m_c))^{1/2}$ with $m_c = 4\pi\rho a^3/3$ (ρ is the density of the particle) we obtain

$$\xi = \frac{\epsilon_0 k_m}{\pi \zeta a^{5/2}} \sqrt{\frac{6k_B T}{\rho}}. \quad (4)$$

Fig. 2 shows typical dependencies of the selection parameter ξ on the particle at the room temperature $T = 298.15$ K for (a) PMMA particles ($\rho = 1180$ kg/m³) suspended in AOT/hexadecane solutions and (b) polystyrene latex particles ($\rho = 1005$ kg/m³) in NaCl aqueous solutions. The values of conductivity (at different salt concentrations) for AOT/hexadecane and KCl/water have been taken from refs. 14 and 18, respectively. It can be seen that in the concentrated solutions the constant potential condition should be applied for almost all values of particle radius, whereas for small particles ($a \ll 1$ μ m) and/or for dilute solutions ($\leq 10^{-2}$ mM) the constant charge condition should be valid.

3 Methodology

When charged particles are sufficiently far apart that they can be considered isolated, each particle acquires a potential corresponding to a zero net current of positive and negative ions (so-called floating potential), thus achieving thermodynamic equilibrium. Provided the particle is uniformly charged the surrounding electric potential does not exhibit any angular dependence, and at low surface potential (less than 25 mV) it can be described by a linearized Poisson-Boltzmann relationship

$$\Delta\Phi_{\text{out}} = \kappa^2\Phi_{\text{out}}, \quad (5)$$

where Φ_{out} is the electric potential outside the particle and κ^{-1} is the Debye length. Eq. (5) is a particular case of the Helmholtz equation, and for the case of spherical symmetry a solution has the following form^{19,20}

$$\Phi_{\text{out}} = \tilde{A}_0 \frac{K_{1/2}(\kappa r)}{\sqrt{\kappa r}}, \quad (6)$$

where \tilde{A}_0 is a constant coefficient, $K_{1/2}(\kappa r)$ is a modified Bessel function of the third kind and r is a radial coordinate with an origin at the centre of the particle. Introducing $A_{0,i} \equiv \sqrt{\frac{\pi}{2}} \frac{\tilde{A}_{0,i}}{\kappa}$ we obtain

$$\Phi_{\text{out}} = \frac{A_0}{r} \exp(-\kappa r). \quad (7)$$

The coefficients $A_{0,i}$ can be found from the boundary condition for the electric field, namely

$$-k_m \left. \frac{\partial\Phi_{\text{out}}}{\partial r} \right|_{r=a+0} = \frac{\sigma}{\epsilon_0}, \quad (8)$$

where σ is the surface charge density. Integrating Eq. (8) over the particle surface yields:

$$A_0 = \frac{Q \exp(\kappa a)}{4\pi\epsilon_0 k_m (1 + \kappa a)}, \quad (9)$$

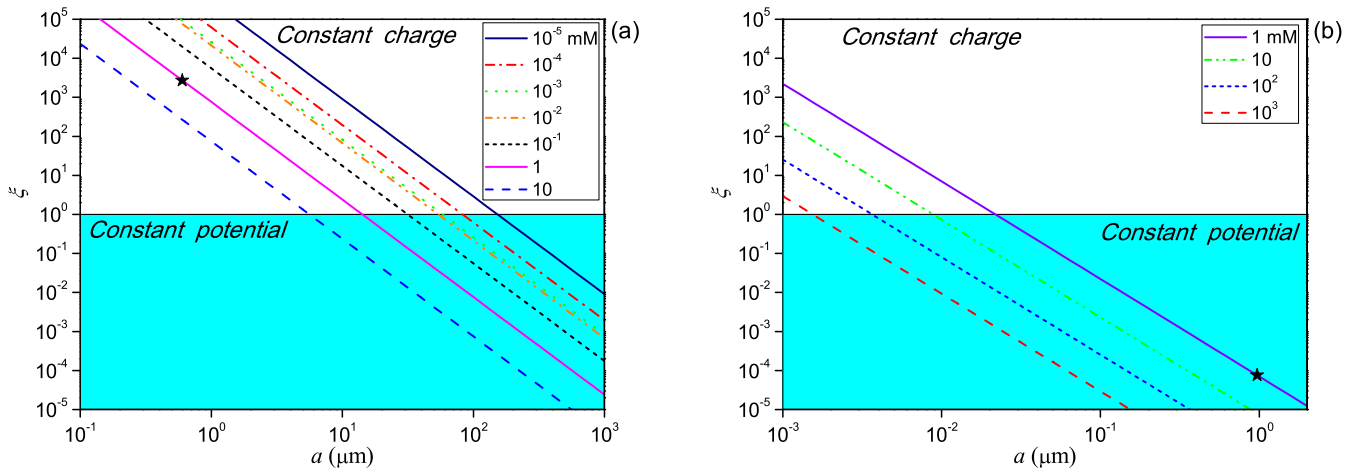


Fig. 2 The selection parameter ξ as a function of the particle radius a for two types of colloidal particles suspended in electrolyte solutions at different molar concentrations of electrolyte at $T = 298.15$ K: (a) PMMA particles ($\rho = 1180$ kg/m³) in AOT/hexadecane solution and (b) polystyrene latex particles ($\rho = 1005$ kg/m³) in KCl/water solution. Points denoted by ‘★’ correspond to the experimental data considered in section 5.

where $Q = \oint \sigma ds$ is the total charge on the particle. Hence, the surface potential takes the following form:

$$\Phi_{\text{surface}} \equiv \Phi_{\text{out}}(a) = \frac{Q}{4\pi\epsilon_0 k_m a (1 + \kappa a)}. \quad (10)$$

Within the Debye-Hückel approximation, at screening lengths comparable to the particle radius, i.e. $\kappa a \gg 1$, Eq. (10) can be simplified to the Graham equation as follows:¹

$$\sigma = \frac{1 + \kappa a}{a} \epsilon_0 k_m \Phi_{\text{surface}} \approx \epsilon_0 k_m \kappa \Phi_{\text{surface}}. \quad (11)$$

Note that Eq. (11) provides a relationship between surface charge and surface potential for an *isolated* particle.

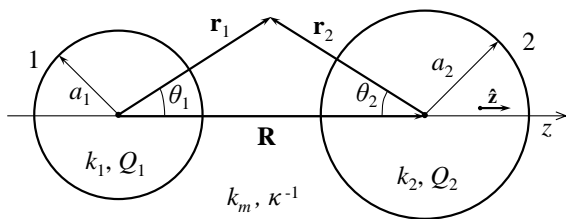


Fig. 3 A general geometry representation of the problem of two interacting, dissimilar colloidal particles in an electrolyte solution with a dielectric constant k_m and a Debye length of κ^{-1} . Dielectric constants, surface charges, and the radii of particles 1 and 2 are denoted as k_1 , Q_1 , a_1 , and k_2 , Q_2 , a_2 , respectively.

According to the model developed previously for two interacting particles^{10,11} (see Fig. 3) the total potential at the boundary of the i -th sphere ($i = 1, 2$) is given by

$$\begin{aligned} \Phi_{\text{out}}(\tilde{a}_i, \mu_i) &\equiv \Phi_{\text{out},i}(\tilde{a}_i, \mu_i) + \Phi_{\text{out},j}(\tilde{a}_i, \mu_i) \\ &= \sum_{n=0}^{\infty} \left[A_{n,i} \frac{K_{n+1/2}(\tilde{a}_i)}{\sqrt{\tilde{a}_i}} + \sum_{l=0}^{\infty} b_{nl}(\tilde{a}_i, \tilde{R}) A_{l,j} \right] P_n(\mu_i), \end{aligned} \quad (12)$$

where $\tilde{a}_i = \kappa a_i$, $\tilde{R} = \kappa R$, $A_{n,i}$ and $A_{l,j}$ are constant coefficients that can be found from boundary conditions, $b_{nl}(\tilde{a}_i, \tilde{R})$ are the re-expansion coefficients of $\Phi_{\text{out},j}(\tilde{a}_i, \mu_i)$ defined below, $P_n(\mu_i)$ are Legendre polynomials, $\mu_i = \cos \theta_i$, and $j = 3 - i$. Therefore, the

boundary condition for constant surface potential takes the form:

$$\sum_{n=0}^{\infty} \left[A_{n,i} \frac{K_{n+1/2}(\tilde{a}_i)}{\sqrt{\tilde{a}_i}} + \sum_{l=0}^{\infty} b_{nl}(\tilde{a}_i, \tilde{R}) A_{l,j} \right] P_n(\mu_i) = \Phi_{\text{surface},i}, \quad (13)$$

and the coefficients are defined as follows:^{10,11}

$$\begin{aligned} b_{nl}(\tilde{a}, \tilde{R}) &= (2l - 1)!! \sum_{m=0}^{\infty} \sum_{k=0}^l (-1)^k \frac{l!}{k!(l-k)!} \\ &\times \frac{\Omega_{l+m+1/2}(\tilde{a}, \tilde{R})}{\tilde{R}^k \tilde{a}^{l-k}} \sum_{l=0}^k \lambda_{kl} \sum_{v=0}^m \gamma_{m lv} p_{v+l,n}, \end{aligned} \quad (14)$$

where

$$\Omega_{l+1/2}(\tilde{a}, \tilde{R}) = \sqrt{2\pi} \left(l + \frac{1}{2} \right) \frac{K_{l+1/2}(\tilde{R}) I_{l+1/2}(\tilde{a})}{\tilde{R}^{1/2} \tilde{a}^{1/2}}, \quad (15)$$

$I_{l+1/2}(\tilde{a})$ are modified Bessel functions of the first kind, λ_{kl} and $\gamma_{m lv}$ are the expansion coefficients of Legendre and Gegenbauer polynomials in terms of μ^v , respectively, and $p_{v+l,n}$ are the coefficients of μ^v expansion in terms of Legendre polynomials (for more details, see refs. 10, 11). Eq. (13) can be rewritten in linear form:

$$A_{n,i} \frac{K_{n+1/2}(\tilde{a}_i)}{\sqrt{\tilde{a}_i}} + \sum_{l=0}^{\infty} b_{nl}(\tilde{a}_i, \tilde{R}) A_{l,j} = \Phi_{\text{surface},i} \delta_{n,0}. \quad (16)$$

The interaction force acting on each sphere can then be calculated using the Maxwell stress tensor and is expressed as follows:^{10,11}

$$\begin{aligned} F_{1z} &= 4\pi\epsilon_0 k_m \sum_{n=1}^{\infty} \frac{n}{(2n-1)(2n+1)} \\ &\times [\Xi_{n-1} - (n-1)\Psi_{n-1}] [\Xi_n + (n+1)\Psi_n], \end{aligned} \quad (17)$$

where

$$\begin{aligned} \Xi_n &= A_{n,i} \frac{n K_{n+1/2}(\tilde{a}_1) - \tilde{a}_1 K_{n+3/2}(\tilde{a}_1)}{\tilde{a}_1^{1/2}} + \tilde{a}_1 \sum_{l=0}^{\infty} A_{l,j} \frac{\partial b_{nl}(\tilde{a}_1, \tilde{R})}{\partial \tilde{a}_1}, \\ \Psi_n &= A_{n,i} \frac{K_{n+1/2}(\tilde{a}_1)}{\sqrt{\tilde{a}_1}} + \sum_{l=0}^{\infty} b_{nl}(\tilde{a}_1, \tilde{R}) A_{l,j}. \end{aligned} \quad (18)$$

Substituting (16) and (18) into (17) gives $\Psi_n = 0$ which leads to

a simplified equation for the electrostatic force:

$$F_{\text{es}} \equiv F_{1z} = 4\pi\epsilon_0 k_m \sum_{n=1}^{\infty} \frac{n}{(2n-1)(2n+1)} \Xi_{n-1} \Xi_n. \quad (19)$$

In order to validate the obtained solution and show the physical significance of the first two terms in Eq. (19), namely,

$$F_{1z} = 4\pi\epsilon_0 k_m \frac{1}{3} \Xi_0 \Xi_1, \quad (20)$$

we consider two limiting cases corresponding to long and short Debye lengths^{10,11} The surface charge distribution can be found using the boundary condition on the normal component of the electric field:

$$-k_m \kappa \frac{\partial \Phi_{\text{out}}(\tilde{a}_i, \mu_i)}{\partial \tilde{a}_i} = \frac{\sigma_i(\mu_i)}{\epsilon_0}. \quad (21)$$

Expansion of Eq. (21) in terms of Legendre polynomials immediately gives the angular distribution of surface charge density:

$$\begin{aligned} \sigma_i(\cos \theta_i) &= -\epsilon_0 k_m \kappa \\ &\times \sum_{n=0}^{\infty} \left[A_{n,i} \frac{n K_{n+1/2}(\tilde{a}_i) - \tilde{a}_i K_{n+3/2}(\tilde{a}_i)}{\tilde{a}_i^{3/2}} + \sum_{l=0}^{\infty} A_{l,j} \frac{\partial b_{0l}(\tilde{a}_i, \tilde{R})}{\partial \tilde{a}_i} \right] P_n(\cos \theta_i). \end{aligned} \quad (22)$$

Integration of Eq. (22) over the surface of the particle yields a total surface charge:

$$Q_i(\tilde{a}_i, \tilde{R}) = 4\pi a_i^2 \epsilon_0 k_m \kappa \left[A_{0,i} \frac{K_{3/2}(\tilde{a}_i)}{\tilde{a}_i^{1/2}} - \sum_{l=0}^{\infty} A_{l,j} \frac{\partial b_{0l}(\tilde{a}_i, \tilde{R})}{\partial \tilde{a}_i} \right]. \quad (23)$$

4 Model verification

4.1 Long Debye length

This first case corresponds to Debye lengths that are much greater than either the radius of a particle or the particle-particle separation: $\kappa a_i \ll \kappa(R - a_1 - a_2) \ll 1$. For small values of the argument, modified Bessel functions of the first and third kind have the following approximate forms:²⁰

$$\begin{aligned} K_{n+1/2}(z) &= \sqrt{\frac{\pi}{2z}} \exp(-z) \sum_{l=0}^n \frac{(n+l)!}{l!(n-l)!(2z)^l}, \\ I_{n+1/2}(z) &\approx \sqrt{\frac{2}{\pi}} \frac{z^{n+1/2}}{(2n+1)!!}, \quad z \ll 1. \end{aligned} \quad (24)$$

The coefficients (14) are approximated as:¹⁰

$$\begin{aligned} b_{00} &\approx \sqrt{\frac{\pi}{2}} \frac{1}{\tilde{R}} \exp(-\tilde{R}), & b_{01} &\approx \sqrt{\frac{\pi}{2}} \frac{1+\tilde{R}}{\tilde{R}^2} \exp(-\tilde{R}), \\ b_{10} &\approx \tilde{a} \sqrt{\frac{\pi}{2}} \frac{1+\tilde{R}}{\tilde{R}^2} \exp(-\tilde{R}), & b_{11} &\approx 0. \end{aligned} \quad (25)$$

Substitution of Eq. (25) into the linear system, Eq. (16), gives:

$$\begin{aligned} A_{0,i} &\approx \sqrt{\frac{2}{\pi}} \frac{\tilde{a}_i}{e^{-\tilde{a}_i}} \Phi_{\text{surface},i}, \\ A_{1,i} &\approx -\frac{\tilde{a}_i^2}{\tilde{R}^2} \frac{1+\tilde{R}}{1+\tilde{a}_i} \exp(-\tilde{R} + \tilde{a}_i) A_{0,j}. \end{aligned} \quad (26)$$

Combining (18), (20), (25), and (26) yields an equation for the force that is well-known from DLVO theory:⁴⁻⁶

$$F_{1z} \approx -4\pi\epsilon_0 k_m \tilde{a}_1 \tilde{a}_2 \frac{1+\tilde{R}}{\tilde{R}^2} \Phi_{\text{surface},1} \Phi_{\text{surface},2} \exp(-\tilde{R} + \tilde{a}_1 + \tilde{a}_2). \quad (27)$$

For two spheres of the same size, Eq. (27) together with Eq. (10) yield an equation for the force between two small ions:^{1,5}

$$F_{1z} \approx -\frac{Q_1 Q_2}{4\pi\epsilon_0 k_m R^2} \frac{(1 + \kappa R) \exp[-\kappa(R - 2a)]}{1 + 2\kappa a}. \quad (28)$$

4.2 Short Debye length

This second case corresponds to both a short particle-particle separation and a short Debye length when compared to particle radii, i.e., $\kappa a_i \gg \kappa(R - a_1 - a_2) \gg 1$. This case is particularly significant for many experiments that involve micron sized colloidal particles and salt concentrations in the region of 1 mM, where the Debye length can equal several nm.^{2,21,22} Modified Bessel functions of the first and third kind have the following asymptotic forms for large values of the argument:²⁰

$$\begin{aligned} K_{n+1/2}(z) &\approx \sqrt{\frac{\pi}{2z}} \exp(-z), \\ I_{n+1/2}(z) &\approx \sqrt{\frac{1}{2\pi z}} \exp(z), \quad z \gg 1. \end{aligned} \quad (29)$$

The coefficients in Eq. (14) then approximate as:

$$\begin{aligned} b_{00} &\approx \sqrt{\frac{\pi}{2}} \frac{\exp(-\tilde{R} + \tilde{a})}{2\tilde{R}\tilde{a}}, & b_{01} &\approx \sqrt{\frac{\pi}{2}} \frac{3\exp(-\tilde{R} + \tilde{a})}{2\tilde{R}\tilde{a}^2}, \\ b_{10} &\approx \sqrt{\frac{\pi}{2}} \frac{3\exp(-\tilde{R} + \tilde{a})}{2\tilde{R}\tilde{a}}, & b_{11} &\approx 0. \end{aligned} \quad (30)$$

Substitution of (30) into the linear system (16) gives:

$$\begin{aligned} A_{0,i} &\approx \sqrt{\frac{2}{\pi}} \tilde{a}_i \exp(\tilde{a}_i) \Phi_{\text{surface},i}, \\ A_{1,i} &\approx -\frac{3}{2} \frac{\exp(-\tilde{R} + 2\tilde{a}_i)}{\tilde{R}} A_{0,j}. \end{aligned} \quad (31)$$

Combining (18), (20) and (31) yields:

$$F_{1z} \approx -4\pi\epsilon_0 k_m \frac{\tilde{a}_1 \tilde{a}_2}{\tilde{R}} \Phi_{\text{surface},1} \Phi_{\text{surface},2} \exp(-\tilde{R} + \tilde{a}_1 + \tilde{a}_2). \quad (32)$$

For two identical spheres, Eq. (32) becomes the well-known equation based on the Derjaguin approximation:^{1,5}

$$F_{1z} \approx -2\pi\kappa a \epsilon_0 k_m \Phi_{\text{surface}}^2 \exp[-\kappa(R - 2a)]. \quad (33)$$

It is interesting to note that in the limit $\kappa a_i \gg \kappa(R - a_1 - a_2) \gg 1$, Eqs. (27) and (28) reduce to Eqs. (32) and (33) respectively.

5 Experimental verification

An examination of these two limiting cases clearly demonstrates that Eq. (19) provides a theoretical description for the behaviour of dielectric particles in an electrolyte solution, under conditions which embrace a wide range of experimental conditions. As a further test for the model, comparisons have been made with two experimental studies. The first comparison is with force measurements taken from optical trap experiments on polymer particles by Sainis *et al.*¹⁴ and the second study examines force measurements taken from cantilever experiment on polystyrene particles by Montes *et al.*²

5.1 Long Debye length – Sainis *et al.*¹⁴

These experiments have been performed on pairs of polymethylmethacrylate (PMMA) spheres of radius 600 nm held in

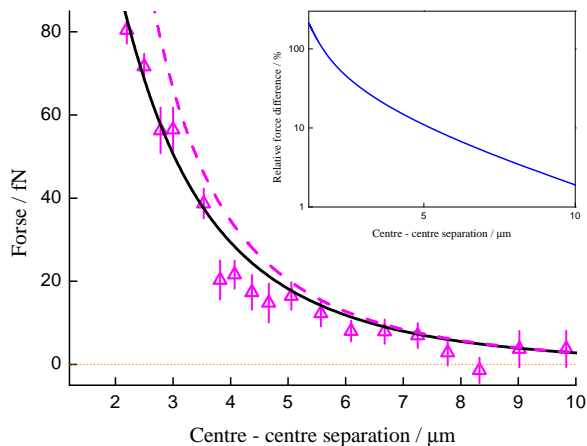


Fig. 4 Electrostatic force between two identical PMMA particles of radius 600 nm in hexadecane ($k_m = 2.06$) with 1 mM of AOT. The symbols are the experimental data. The solid line represents the fitted force calculated within the present model, Eq. (19), and the dashed line corresponds to the force calculated from DLVO theory (27) with the same fitting parameters: Debye length $\kappa^{-1} = 5 \mu\text{m}$ and the particle surface potential $\Phi_{\text{surface}} = 80 \text{ mV}$. The embedded plot shows the relative difference between the exact and approximated force.

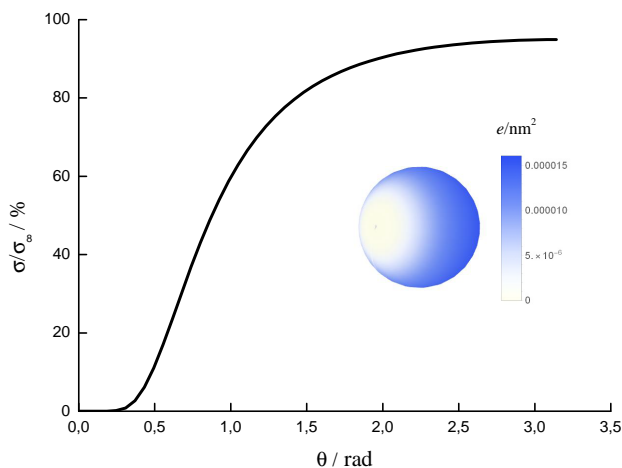


Fig. 5 Surface charge distribution on a PMMA sphere of radius 600 nm in hexadecane with 1 mM of AOT at zero surface-to-surface separation in relation to the surface charge density of an isolated particle.

an optical trap in the presence of a nonpolar solvent (hexadecane) and a charge control agent (AOT). The electrostatic force has been measured for different molar concentrations of AOT equating to different values of particle charge and Debye length. According to Fig. 2a, at AOT concentration 1 mM the boundary conditions of constant charge should be used as it was done in ref. 10. However, the boundary conditions of constant potential are applied here to demonstrate the effect of boundary conditions on fitting parameters and the difference between the results of

the presented model and DLVO theory. Comparison between the experimental data and forces calculated using both Eq. (19) and Eq. (27) (DLVO theory), are shown in Fig. 4. The Debye length $\kappa^{-1} = 5 \mu\text{m}$ and the particle potential $\Phi_{\text{surface}} = 80 \text{ mV}$ (corresponding to a total surface charge $Q = 80 e$) have been taken in order to fit the force given by Eq. (19) to the experimental data; those same parameters have then been used in Eq. (27). The discrepancy between the two force calculations is plotted as a percentage in the insert to Fig. 4. It can be seen that differences between the two forces becomes very evident at separations of about the Debye length and that at the point of contact, they two results differ by almost 200%. Unlike the constant charge case,¹⁰ where the discrepancy is caused by polarization effects at short separation (outside the range of experimental measurements), the constant potential boundary condition implies two effects: first, in accordance with Eq. (22), surface charge is redistributed as the inter-particle separation changes; second, the total charge also changes with inter-particle separation as described by Eq. (23). Fig. 5 shows the surface charge distribution at the point of contact plotted as a ratio to the surface charge density of an isolated particle as calculated from Eq. (11). The charge redistribution is caused by the equilibrium ionic flux and the process of dissociation and recombination of surface groups on a particle. As a consequence of using Eq. (19), both fitting parameters ($\kappa^{-1} = 5 \mu\text{m}$, $Q = 80 e$) are different from those ($\kappa^{-1} = 7 \mu\text{m}$, $Q = 63 e$) found by Sainis *et al.*¹⁴ in their fit to the electrostatic force using the DLVO model; Eq. (27).

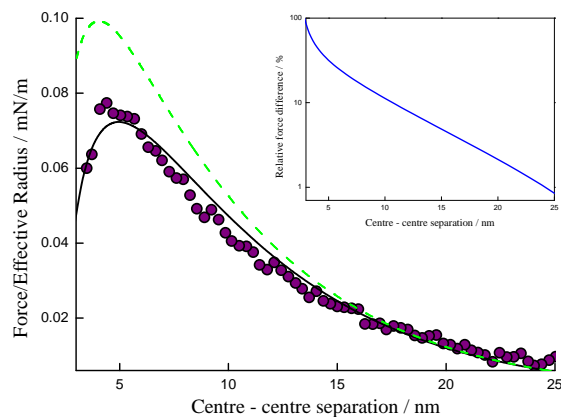


Fig. 6 Force in a symmetric system involving particles of radius $0.97 \mu\text{m}$ at pH 3.0 and a KCl concentration of 1 mM. Points are experimental data and the solid line is the force calculated from Eq. (35) and (19), the dashed line is the force from DLVO theory calculated from Eq. (35) and (32) with the same fitting parameters: the Debye length is $\kappa^{-1} = 6.9 \text{ nm}$, the particle surface potential is $\Phi_{\text{surface}} = 14 \text{ mV}$. The embedded plot shows the relative difference between the exact and approximated force.

5.2 Short Debye length – Montes Ruiz-Cabello *et al.*²

In their experimental study of the electrostatic force between pairs of charged latex particles, Montes Ruiz-Cabello *et al.*² recorded data at different pH values and KCl salt concentrations

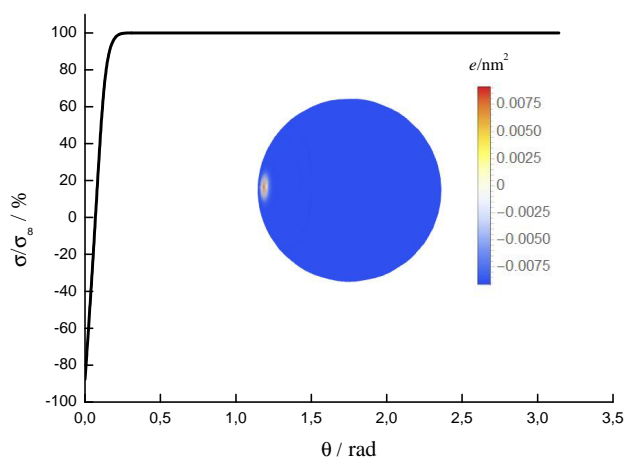


Fig. 7 Surface charge distribution on a polystyrene latex sphere of radius $0.97 \mu\text{m}$ in water with 1 mM of KCl, a pH of 3.0 and at 3 nm surface-to-surface separation in relation to the surface charge density on an isolated particle.

for particles with radii of 0.97 , 0.51 and $1.50 \mu\text{m}$. Fig. 2b reveals that at salt concentration 1 mM the boundary conditions of constant potential should be applied for particle radii greater than $0.1 \mu\text{m}$. For this second validation of the model, data taken for the particle radius of $0.97 \mu\text{m}$ have been chosen as their surface potential is below the thermal energy and, therefore, the Debye-Hückel approach is applicable. In addition to the electrostatic contribution to the force, the van der Waals force has also been taken into account, as given by Montes *et al.*² using the Derjaguin approximation:^{1,5}

$$F_{\text{vdW}} = -\frac{a_1 a_2}{a_1 + a_2} \frac{H}{6(R - a_1 - a_2)^2}, \quad (34)$$

where $H = 4.0 \times 10^{21} \text{ J}$ is the Hamaker constant determined from force profiles. Therefore, the resulting force takes the following form:

$$F_{\text{total}} = F_{\text{es}} + F_{\text{vdW}}. \quad (35)$$

Here F_{es} is the electrostatic force calculated either from Eq. (19) or from its approximation, Eq. (32), and F_{vdW} is the van der Waals force calculated from Eq. (34). We consider the symmetric case of two identical particles. A comparison between the experimental data and the force calculated using Eq. (35) is shown in Fig. 6. The potential is set to be equal to 14 mV which equates to the ζ -potential,² and the Debye length has been calculated from:²³

$$\kappa^2 = \frac{2N_A e^2 I}{\epsilon_0 k_m k_B T}, \quad (36)$$

where N_A is the Avogadro constant, e is the elementary charge, I is the ionic strength, k_B is the Boltzmann constant, and T is the temperature of the solution. For the given conditions, i.e. KCl and HCl concentrations (at pH = 3.0) 1 mM and $T = 298.25 \text{ K}$, the Debye length is approximately 6.9 nm . The results show that at inter-particle separations exceeding the Debye length the experi-

mental results are correctly described within the present model (Eq. (19)). The discrepancy between the force from Eq. (19) and its approximation from DLVO theory (Eq. (32)) can reach up to 100% at close separations, and a difference of less than 10% starts at distances of 2-3 Debye lengths. Fig. 7 shows the surface charge distribution at the point of contact in relation to the surface charge density on an isolated particle (Eq. (11)). Unlike the case for long Debye lengths, the strong screening effect leads to a very narrow area of charge non-uniformity close to the second particle.

6 Conclusion

The electrostatic problem for two colloidal particles in an electrolyte solution has been solved within the Debye-Hückel approximation using the boundary condition of constant potential. This condition generally corresponds to Debye lengths much less than particle size and high concentrations of electrolyte. The force is expressed as an infinite series, and as part of the validation process, it is shown that limiting forms of the first two terms yield known literature expressions for sphere-sphere interactions. It is also shown that the present methodology can be used to interpret current data taken from experiments on colloids for a range of different solvent conditions. The results yield accurate fitting parameters of charge and the screening length, and show how existing approximations fails at short inter-particle distances.

When taken together with a model previously developed for constant surface charge, this new theory, based on a rigorous solution to the electrostatic problem for two spheres in an electrolyte solution, provides a unified approach to the understanding of pairwise electrostatic interactions between spherical colloidal particles. It is shown to be a good alternative to the constant regulation approximation as the latter introduces an additional parameter for charge regulation and relies on the Derjaguin geometric approximation. Finally, the methodology provides a strong link between colloidal systems, dusty plasmas and other complex arrangements involving charged particles.²⁴

Acknowledgements

ERC Consolidator grant (ERC-2012-StG 307755 FIN), Innovate UK grant (102696) and International Space Science Institute (Bern) support are gratefully acknowledged. I.N.D and A.V.F. also acknowledge support in part by a grant from the Russian Science Foundation (16-12-10424). AJS would like to thank the Leverhulme Trust for the award of an Emeritus Fellowship. The authors are thankful to Professors Eric Dufresne and Michal Borkovec, and Doctor Plinio Maroni for providing the raw experimental data.

References

- [1] J. N. Israelachvili, *Intermolecular and Surface Forces*, Elsevier Inc., Waltham, MA, USA, 3rd edn, 2011.
- [2] F. J. Montes Ruiz-Cabello, P. Maroni and M. Borkovec, *J. Chem. Phys.*, 2013, **138**, 234705.
- [3] B. Derjaguin and L. Landau, *Acta Physicochim. USSR*, 1941, **14**, 58.
- [4] E. J. W. Verwey and J. T. G. Overbeek, *Theory of Stability of Lyophobic Solids*, Elsevier, Amsterdam, 1948.

- [5] B. Derjaguin, *Trans. Faraday Soc.*, 1940, **35**, 203.
- [6] A. V. Filippov, I. N. Derbenev, A. A. Pautov and M. M. Rodin, *J. Exp. Theor. Phys.*, 2017, **125**, 518.
- [7] R. Hogg, T. Healy and D. Fuerstenau, *Trans. Faraday Soc.*, 1966, **62**, 1638.
- [8] S. Carnie and D. Chan, *Colloid Interface Sci.*, 1993, **161**, 260.
- [9] R. Pericet-Camara, G. Papastavrou, S. Behrens and M. Borkovec, *J. Phys. Chem. B*, 2004, **108**, 19467.
- [10] I. N. Derbenev, A. V. Filippov, A. J. Stace and E. Besley, *J. Chem. Phys.*, 2016, **145**, 084103.
- [11] A. V. Filippov and I. N. Derbenev, *J. Exp. Theor. Phys.*, 2016, **123**, 1099.
- [12] E. Bichoutskaia, A. L. Boatwright, A. Khachatourian and A. Stace, *J. Chem. Phys.*, 2010, **133**, 024105.
- [13] V. R. Munirov and A. V. Filippov, *J. Exp. Theor. Phys.*, 2013, **117**, 809.
- [14] S. K. Sainis, J. W. Merrill and E. R. Dufresne, *Langmuir*, 2008, **24**, 13334.
- [15] J. A. Stratton, *Electromagnetic Theory*, McGraw-Hill, New York, 1941.
- [16] A. V. Filippov, *J. Exp. Theor. Phys.*, 2009, **109**, 516.
- [17] A. V. Filippov, *Contributions to Plasma Physics*, 2009, **49**, 431.
- [18] *Electrolytic conductivity measurement: Theory & Application*, Aquarius Technical Bulletin, No. 8, Aquarius Technologies, 2009.
- [19] P. Morse and H. Feshbach, *Methods of Theoretical Physics, Part II*, McGraw-Hill, New York, 1953.
- [20] G. N. Watson, *A treatise on the theory of Bessel functions*, Cambridge university press, 1966.
- [21] D. Murakami, A. Takenaka, M. Kobayashi, H. Jinnai and A. Takahara, *Langmuir*, 2013, **29**, 16093.
- [22] M. M. Elmahdy, C. Gutsche and F. Kremer, *J. Phys. Chem. C*, 2010, **114**, 19452.
- [23] P. Debye and E. Hückel, *Phys. Z.*, 1923, **24**, 185.
- [24] V. E. Fortov, A. G. Khrapak, S. A. Khrapak, V. I. Molotkov and O. F. Petrov, *Phys.-Usp.*, 2004, **47**, 447.